Published in final edited form as:
Nat Struct Mol Biol. 2009 March ; 16(3): 238–246. doi:10.1038/nsmb.1558.

PHOSPHORYLATION-MEDIATED UNFOLDING OF A KH DOMAIN REGULATES KSRP LOCALISATION VIA 14-3-3 BINDING

Irene Díaz-Moreno[1,5,*], **David Hollingworth**[1,*], **Thomas A. Frenkiel**[2], **Geoff Kelly**[2], **Stephen Martin**[3], **Steven Howell**[1], **MaríaFlor García-Mayoral**[1], **Roberto Gherzi**[4], **Paola Briata**[4], and **Andres Ramos**[1]

[1]Molecular Structure Division, MRC National Institute for Medical Research, The Ridgeway, Mill Hill, London NW7 1AA, UK.

[2]MRC Biomedical NMR Centre, The Ridgeway, Mill Hill, London NW7 1AA, UK.

[3]Physical Biochemistry Division, MRC National Institute for Medical Research, The Ridgeway, Mill Hill, London NW7 1AA, UK.

[4]Istituto Nazionale per la Ricerca sul Cancro, Largo Benzi Rosanna, 10, Genova 16132, Italy.

[5]Istituto de Bioquimica Vegetal y Fotosintesis, US-CSIC, Avda. Amerigo Vespucio 49, 41092, Sevilla, Spain

Abstract

The AU-rich-element (ARE)–mediated mRNA degradation activity of the RNA-binding K-homology Splicing Regulator Protein (KSRP) is regulated by phosphorylation of a serine within its N-terminal KH domain (KH1). In the cell phosphorylation promotes the interaction between KSRP and 14-3-3ζ protein and impairs the ability of KSRP to promote the degradation of its RNA targets. Here we examine the molecular details of this mechanism. We report that phosphorylation leads to the unfolding of the structurally atypical and unstable KH1, creating a site for 14-3-3 binding. Using this site 14-3-3 discriminates between phosphorylated and non phosphorylated KH1, driving the nuclear localization of KSRP. 14-3-3–KH1 interaction regulates the mRNA decay activity of KSRP by sequestering the protein in a separate functional pool. This study demonstrates how an mRNA degradation pathway is connected to extra cellular signaling networks by the reversible unfolding of a protein domain.

INTRODUCTION

Gene regulation by adenosine-uridine-rich element (ARE)-mediated mRNA decay (AMD) is important for physiological cellular proliferation, immune response and cardiovascular toning. Indeed AMD malfunction has been linked to cancer[1] and to inflammatory diseases

Correspondence should be addressed to A.R. (aramos@nimr.mrc.ac.uk).
*These authors contributed equally to the work

AUTHOR CONTRIBUTIONS

Cloning and site-specific mutagenesis was performed by D.H. Protein purification of was performed by I.D.M. and D.H. NMR experiments were performed by I.D.M., G.K., T.A.F. and A.R. NMR data analysis was performed by I.D.M. and M.G.M. Structure calculations were performed by I.D.M. CD experiments and analysis of CD data were performed by A.R. and S.M. Mass spectrometry analysis was performed by S.H. Phosphorylation experiments were designed and carried out by D.H. ITC experiments were performed by A.R.. Sub-cellular localization experiments were performed by L.B. and R.G. The paper was written by I.D.M.. and A.R.

Note: Supplementary information is available on the Nature Structural & Molecular Biology website.

CONFLICT OF INTEREST STATEMENT

The authors declare no conflict of interest.

such as Crohn-like inflammatory bowel disease and inflammatory arthritis2. The effect of *cis*-acting AREs on the stability of specific mRNAs is mediated by the binding of regulatory proteins (ARE-binding proteins, ARE-BPs). Some of these proteins (e.g. TPP, BRF1, KSRP) promote mRNA degradation while others (e.g. HuD and HuR) act antagonistically, stabilizing the mRNA[3]. The rate of decay of these mRNAs is therefore controlled by the interplay between different protein effectors.

K-homology splicing regulator protein/fuse binding protein 2 (KSRP/FBP2) is an important ARE-BP (also called turnover and translation regulatory BPs (TTR-BPs[4]), that has been shown to recruit the exosome to a subset of mRNA targets, promoting their degradation[5,6]. The central part of the protein is organized in four single stranded nucleic acid binding domains, the so-called K-homology domains (Figure 1a, KH1 to 4). Using cross-linking and mRNA decay assays, we have shown that the third and fourth KH domain of KSRP are required for mRNA binding and degradation[6]. We have also examined the ability of KH3 and KH4 to bind AU-rich sequences using *in vitro* biophysical assays; this study clarified that binding by more than one domain is necessary to attain high affinity[7].

Recently two independent phosphorylation events that link KSRP-mediated mRNA degradation to extra cellular regulatory networks have been identified8,9. Phosphorylation of a threonine in the C-terminal region of KSRP (Thr692) by p38 MAPK is necessary to regulate the decay of ARE-containing myogenic mRNAs[8], while phosphorylation of a serine (Ser193, Figure 1b) within the first KH domain of KSRP by AKT/PKB kinase reduces the degradation rate of a subset of mRNAs encoding RNA binding proteins, signalling molecules and a replication-independent histone[9,10]. The two phosphorylation events are regulated by different pathways and produce distinct molecular effects. While Thr692 phosphorylation mediates a change in the ARE binding capabilities of KSRP[8], Ser193 phosphorylation does not influence directly the binding to the target AREs but prevents KSRP from recruiting the exosome[9].

We have previously shown that the impairment of exosome recruitment is mediated by the binding of the 14-3-3ζ protein to the Ser193-phospho-KSRP9. 14-3-3 is a ubiquitous regulatory protein that has been reported to bind more than 100 targets, most of them phosphorylated linear peptidic chains within larger proteins11¯14. In the most common mode of interaction the phosphorylated amino acid and a few neighbouring residues lay along the concave surface of 14-3-3 in an extended conformation and are recognised by the side chains of the protein residues. This interaction can be disrupted by specific inhibitors (e.g. difopein) that can be used to confirm the relevance of 14-3-3–target interactions in a range of regulatory processes. Interestingly, 14-3-3 has been shown to regulate stress granule formation and mRNA decay when associated with the phosphorylated ARE-BP TTP15. The 14-3-3 TTP target sequence is closely related to that of KSRP16, but it is located in an unfolded area of the protein and not, as in the case of KSRP, within an RNA-binding domain. KSRP Ser193 lies within the sequence boundaries of the first KH domain (KH1) and a conformational rearrangement may be necessary to allow the recognition of the phospho-serine and the neighbouring amino acids by 14-3-3.

In order to understand the effect of Ser193 phosphorylation at the molecular level, we have determined the structure and dynamics of human KSRP KH1 and defined its relationship with the other domains of the protein and with the AU-rich RNA targets. We have then probed the structural changes caused by phosphorylation of Ser193 *in vitro* using NMR spectroscopy and showed that phosphorylation destabilises the domain, creating a binding site for 14-3-3. The mechanism of phosphorylation and role of the phosphate group are analysed with the help of data on the conformation/stability of a phospho-mimic S193D mutant and a control S193A mutant. We also show that phospho-KH1 interacts directly and

specifically with 14-3-3 *in vitro* and phosphorylation of Ser193 causes a 14-3-3-dependent alteration of the nuclear/cytoplasmic distribution of the protein. Our work indicates that KH1 acts as a switch in the mRNA decay activity of KSRP by shifting the protein between distinct sub-cellular pools, and leads to a novel regulatory model that may be applicable to other 14-3-3 targets.

RESULTS

KH1 structure, inter-domain interactions and RNA recognition

The solution structure of KSRP KH1 (Ile130–Gly218) contains a classical KH fold, with three α-helices packed against a three-stranded anti-parallel β sheet in a βααββα topology (Figure 2a, b) typical of the eukaryotic KH type 1 family. This canonical KH fold is well defined by the NOE data except for the GXXG and variable loops. These loops undergo motions on millisecond and nano-to-picosecond timescales respectively that have been linked with the RNA binding ability of the domain[17-19].

In KH1, the central KH core is extended by a novel thirteen-residue N-terminal element that folds back to form a short anti-parallel fourth strand (β_0) and augments the exposed surface of the sheet, reaching the proximity (4-5 amino acids) of the bi-partite Nuclear Localization Signal (NLS) of KSRP (Figure 1a) .A self-consistent set of individually assigned long range NOE cross-peaks between this conserved (Figure 1b) N-terminal extension and the core KH fold - including the correlations between Ser132 HN and Glu148 HN and Gln133 Hα and Glu147 Hα - was instrumental in packing the strand against the core KH domain. Addition of β_0 is consistent with the appreciable difference in the global rotational correlation time (τ_c) of KH1 with and without the N-terminal extension (6.5 ns *versus* 5.1 ns, respectively; Supplementary Table 1a) and contrasts with the much smaller (0.6-0.7 ns) increase in τ_c observed upon addition of the longer KH12 linker to either KH1 or KH2 (Supplementary Table 1a). However, nano-to-picosecond motions are observed for the N-terminal extension (Supplementary Fig. 1a) hinting at substantial flexibility.

The interaction between the canonical β-sheet and the N-terminal extension, is stabilized by a network of H-bonds involving residues of β_0, of β_1 and of the β_0-to-β_1 turn ($turn_0$) (Figure 2c). However, it does not bury hydrophobic side chains (Figure 2d) and is associated with a very small change in stability, as observed in our CD thermal unfolding studies (Supplementary Figure 1b). A structural homology search using both the DALI server[20] and a local structure-based alphabet[21,22], confirmed that loop-turns structurally similar to the N-terminal extension can be found in very different structural and functional contexts but is observed here for the first time adjacent to a KH domain.

Interactions between neighboring KH domains of the Nus A, Vg1RBP and FMRP proteins[23-25] have been reported to influence their structure and stability. To investigate the possibility of an interaction between KH1 and the other KH domains of KSRP we superimposed the ^{15}N-HSQC NMR spectra of the KH1 and KH2 substantial chemical shift differences, indicates that KH1 and KH2 do not interact in a stable and specific way. Further, KH1 resonances do not change in the four-domain construct indicating that no extra contacts are made in KH1234 (Supplementary Fig. 2). The absence of a stable KH1–KH2 interaction is validated by NMR relaxation data and by thermal unfolding. The trend of ^{15}N T_1 and T_2, and $^{15}N\{^1H\}$ NOE values along the protein sequence (Figure 3b) is similar in KH1, KH2 and KH12 while the 14-residue KH1–KH2 linker is very flexible (Supplementary Fig. 1a). The moderate increase in the rotational correlation time (τ_c) observed in the two-domain construct (Supplementary Table 1a) is not consistent with the two domains tumbling as a stable single unit[26]. Thermal unfolding studies by CD and NMR show that the transition mid-point of KH1 and KH2 unfolding does not change appreciably

in the two-domain construct (Figure 3c, Supplementary Table 1b and data not shown), confirming that $KH1_{130–218}$ is an adequate structural model for our studies. Interestingly, thermal unfolding indicates that KH1 is not only much less stable than KH2 (Supplementary Table 1b) but also substantially less stable than KH3 and KH4[7].

Chemical-shift perturbation mapping showed that the interaction of KH1 with short AU-rich RNA targets[7] does not involve the β_0-$turn_0$ element but occurs within the previously defined[19,27] KH1 canonical nucleic acid binding groove (Supplementary Fig. 3). However, the affinity of the interaction is too low to be accurately measured (K_d higher than 1 mM) and substantially lower of the one of KH2 (K_d = 398 ± 47 μM) (data not shown), KH4 (K_d = 270 ± 30 μM) and KH3 (K_d ~ 125 ± 3 μM) (7) for the same sequences. The low affinity of KH1 for AU-rich sequences indicates that the domain probably plays a secondary role - if any - in ARE recognition.

KH1 phosphorylation acts as a conformational switch

In the KH1 structure Ser193 is positioned in the central part of the β-sheet and it cannot be recognized by 14-3-3ζ in a classical phospho-dependent way. We used NMR to directly test the effect of Ser193 phosphorylation on the conformation of KSRP KH1. We established a simple protocol that allowed us to use commercial AKT enzyme to phosphorylate *wild type* KH1 to ~90% efficiency. We then purified the two (phospho and non-phospho) species using a size exclusion column and analyzed them by mass spectrometry.

Supplementary Fig. 4 shows the chromatogram of a size exclusion column loaded with the phosphorylation reaction and the results of the mass spectrometry analysis of the two peaks. The higher mobility of the phospho-protein is consistent with an increase of apparent protein volume due to the unfolding of the domain. High sensitivity SOFAST ^{15}N-^{1}H HMQC spectra[28] were recorded on samples from the two HPLC peaks (Figure 4a): the two spectra clearly show that the non-phosphorylated protein is folded, while the phosphorylated protein is essentially unfolded. The amide resonances of phosphoKH1 are in the random coil region of the spectrum and show a pH-dependent broadening (Supplementary Fig. 5) typical of exposed amides resonances in exchange with the bulk water. The folding state of phospho-KH1 was confirmed by recording CD spectra at different temperatures (20, 40, 60, 80 and 95 °C) (Figure 4b). The spectrum of the protein does not change with temperature and the analysis of the secondary structure components show that the apparent percentage of unfolded peptidic chain at 20 °C (79.9 %) is in the range expected for fully unfolded proteins (69.8-89.9 %)[29]. The S193A mutant was used as a control: no detectable phosphorylation was observed in a reaction identical to the one described above. Similarly, no phosphorylation or unfolding was observed in a reaction with thermally inactivated kinase and *wild type* protein (data not shown).

In the cell, regulation by phosphorylation is a reversible process. To assess the reversibility of the changes induced by Ser193 phosphorylation, the phosphorylated protein was de-phosphorylated using protein λ phosphatase. A SOFAST ^{15}N-^{1}H HMQC spectrum was recorded on the phosphatase-treated sample, showing that the removal of the phosphate group leads to complete refolding of the protein (Figure 4c).

In order to better dissect the effect of introducing a phosphate group on the structure and stability of KH1 we mutated Ser193 to both alanine and aspartate and used NMR to assess the conformation and stability of the mutants. ^{15}N-^{1}H HSQC experiments recorded on the S193A mutant showed a well-dispersed spectrum similar to that of the KH1 *wild type* construct (Figure 5a). Changes in the spectrum were limited to resonances of amides in the immediate proximity of the mutated residue. Further, thermal unfolding of the mutant was followed by CD which confirmed that its stability is similar to that of the *wild type* domain

(Figure 5b). This indicates that the conserved serine has a functional rather than a structural role. Conversely, mutation of the serine to the phospho-mimic aspartate drastically changed the stability of the protein. The ^{15}N-^{1}H HSQC spectrum of the mutant recorded at 27°C shows that the protein exist as an equilibrium mixture of folded and unfolded species (Figure 5a) and that the spectrum of the folded form is very similar to that of the *wild type* KH1, with changes being consistent with a S193D point mutation. NMR spectra recorded at both lower and higher temperature showed, as expected, a reversible shift of the folded/unfolded equilibrium towards the unfolded species (Supplementary Fig. 6). CD spectra confirmed that the mutant is undergoing both cold and high temperature unfolding and that, even at the point of maximum stability (15°C) only ~70% of the protein is folded (data not shown). Introduction of a negative charged side chain at position 193 severely destabilizes the domain, confirming the role of the phosphate group in domain unfolding.

14-3-3ζ–Phospho-KH1 recognition

Our data indicate that phosphorylation of KH1 unfolds the domain and creates a site for 14-3-3 binding. We wanted to analyze the interaction between 14-3-3ζ protein and the phosphorylated and unfolded KSRP KH1 domain using SOFAST ^{15}N-^{1}H HMQC spectra. Initially we titrated unlabelled 14-3-3 into a sample of unmodified ^{15}N-labelled KH1: no change takes place in the fingerprint spectra of the domain, indicating that the two proteins are not interacting (Figure 6a). In contrast, when unlabelled 14-3-3 is added to the phosphorylated KH1 we observe a strong selective decrease in the intensity of the NMR signal of a small number of resonances (Figures 6a and 6b). This observation is consistent with 14-3-3 interacting with a short target sequence within the phosphorylated domains. We expect that, because of the interaction with the large 14-3-3 protein, the resonances of residues directly involved in the binding would broaden very markedly, possibly beyond detection. Non-neighboring residues that are separated from the 14-3-3 binding site by a flexible stretch of several amino acids would be shielded from the effect of the molecular weight increase and will undergo very moderate broadening. To confirm that this model is applicable to our data and to show that the 14-3-3-KH1 interaction is indeed mediated by a short unfolded and phosphorylated amino acid stretch we have used a 10-fold excess of a phospho-peptide that spans the KH1 14-3-3 target sequence (GLPERSV**S$_p$**LTGAPES) to compete out 14-3-3 protein. Upon addition of the peptide to the 14-3-3-KH1 complex, the KH1 resonances that had undergone selective broadening re-appeared in the spectra (Figures 6a and 6b).

To directly explore the role of the phosphate group in 14-3-3 recognition of the peptidic sequence defined above we have compared the binding of the KH1 phospho and non-phosphopeptides of that sequence to 14-3-3ζ by isothermal titration calorimetry (ITC). Our experiments show that 14-3-3ζ binds to the phosphopeptide with a ~1:1 stoichiometry and 27μM Kd, while no binding is observed for the non phosphorylated peptide (Supplementary Fig. 7). This confirms that the phosphate is directly involved in 14-3-3ζ binding and indicates a binding mode consistent with the inhibitory effect of difopein observed in our functional assays.

The experiments described above show that KH1 interacts with 14-3-3 only when the domain is phosphorylated and unfolded and that, as we previously proposed[9], this interaction is mediated by a short target sequence within the domain.

KSRP phosphorylation leads to nuclear localization

KSRP is known to shuttle between nucleus and cytoplasm in response to extra-cellular stimuli and its nuclear/cytoplasmic distribution varies substantially depending on cell type and conditions[8,9]. 14-3-3ζ is a predominantly nuclear isoform and has been shown to

change the nuclear localization of, among others, the mRNA decay-promoting factor TTP[16]. Therefore we reasoned that binding to 14-3-3ζ may lead to nuclear retention of KSRP and that nuclear localization may be responsible for the inability of the protein to recruit the mRNA degradation machinery. In order to assess the effect of Ser193 phosphorylation on KSRP sub-cellular localization we compared the nucleo/cytoplasm distribution of the protein in pituitary αT3-1 cells stably expressing a constitutively active AKT1 (myrAKT1) and in a mock-transfected αT3-1 negative control[9]. KSRP was similarly distributed in the S100 cytoplasmic and the nuclear fractions in the mock-αT3-1 cells, while it was mainly nuclear in the αT3-myrAKT-1 (Figure 7a). These data were confirmed using HIRc-B cells, in which AKT activation can be induced by insulin treatment (Figure 7b). Here also, AKT activation promotes nuclear localization of KSRP. The expression of a constitutively active AKT as well as the activation of endogenous AKT by insulin treatment did not affect the cellular distribution of the ribo-nucleoproteins AUF1 and hnRNPA1, confirming the specificity of the effect we observe for KSRP (Figure 7). AKT-driven phosphorylation and the resulting interaction with 14-3-3ζ mediate the nuclear localization of KSRP, presumably by sequestering the protein in the nucleus. In order to exclude the involvement of the NLS of KSRP in its AKT-mediated nuclear retention we transiently transfected in HEK293 cells a Flag-tagged KSRP deletion mutant that contains the four KH domains but excludes the NLS. The results presented in Figure 7c indicate that co-expression of myrAKT caused an enrichment of Flag 1-4 in the nuclear compartment. Importantly, the co-expression of difopein[30], a specific inhibitor of the classical 14-3-3-ligand interaction mode, eliminated the effect of KSRP (Figure 7c). Also, myrAKT1 expression did not affect the localization of the Flag-tagged KSRP(S193A) mutant in transiently transfected HEK293 cells (Figure 7d).

Altogether these results highlight the relevance of Ser193 phosphorylation by AKT to the control of the sub-cellular localization of KSRP.

DISCUSSION

Our results describe, for the first time, a phospho-dependent switch based on the unfolding of a KH domain, KH1 of KSRP. AKT phosphorylation of KH1 is responsible for its unfolding, which creates a binding site for 14-3-3. In turn, binding of 14-3-3 results in the increased nuclear localization of KSRP and therefore decreases its mRNA degradation activity in the cytoplasm. This work shows that KH domains can function not only as nucleic acid binding units but as independent regulatory elements and provides a molecular links between a signaling event and mRNA metabolism.

KH1 phosphorylation and 14-3-3 recruitment

The structure of KSRP KH1 reveals that access to Ser193, whose phosphorylation regulates 14-3-3 binding and mRNA decay, is restricted by an N-terminal extension of the domain and by the geometry of the β-sheet. However, competition experiments using difopein[9] suggest that 14-3-3 recognizes KH1 using the extended and accessible stretch of amino acids containing a phosphoserine or phosphothreonine. This apparent contradiction is explained by the unfolding undergone by the protein upon phosphorylation of Ser193 that creates a binding site for 14-3-3. Unfolding is not due to the disruption of specific interactions made by the serine side chain but to a specific role of the negative charged phosphate group. The phosphomimic S193D mutant is also largely unfolded at 37 °C, while the S193A mutant used as a negative control in a previous functional study[9] shows the same stability as the *wild type* protein.

Non-phosphorylated KH1 is not recognized by 14-3-3 while phospho-KH1 interacts with the protein: once KH1 is phosphorylated and unfolded 14-3-3 can recognize the domain. The changes observed in the phospho-KH1 spectrum upon 14-3-3 binding are reversed by

adding a KH1-derived phospho-peptide that contains the 14-3-3 binding site indicating that the key contacts are provided by a short stretch of amino acids including and flanking Ser193. Further - and consistently with our functional data - ITC experiments on the phospho-peptide and its non-phosphorylated version show that only the phospho-peptide binds to 14-3-3ζ and indicate the phosphate group itself is involved in recognition. This does not exclude that other parts of KSRP also interact with 14-3-3. Target dimerisation or binding to additional sites has been observed in 14-3-3–target recognition and the affinity of the phosphopeptide for 14-3-3ζ (27 μM K_d) indicates that secondary contacts are likely to occur *in vivo*.

Structural rearrangement upon phosphorylation is a common regulatory mechanism31, but there are no reported examples, to our knowledge, of a complete unfolding of an RNA binding domain. Phosphorylation of a residue at the boundaries of a KH domain has been reported for the hnRNP K protein, where the Y458D phospho-mimic mutation leads to a change in protein dynamics and a decrease in RNA binding but does not change the structure of the domain[32]. The phosphorylation-mediated unfolding of KH1 represents a novel regulatory mechanism and could be explained by the atypically low stability of KH1. The domain structure shields Ser193 not only from 14-3-3 but also from AKT recognition. However, the appreciable fraction (~16%) of unfolded protein at 37°C facilitates the access of the AKT kinase to the residue to be phosphorylated. Then the phosphorylation event traps KH1 in the unfolded conformation and drives the folded/unfolded equilibrium to the unfolded state. This regulatory mechanism is reversible, as refolding of KH1 can be achieved by de-phosphorylation of the protein by a phosphatase. Proteomics-derived patterns of phosphorylation (Phosphosite® database, http://www.phosphosite.org/) indicate that phosphorylation within the boundaries of a domain is not uncommon for post-transcriptional regulatory factors: the data presented here could indicate that phosphorylation-mediated domain unfolding may be common in the control of post-transcriptional regulatory factors.

Role of KH1 in ARE-mediated mRNA degradation

The *in vitro* RNA binding ability of KSRP is not affected by KH1 phosphorylation[9]. However, we show here that phosphorylation leads to unfolding of KH1 and therefore to the complete disruption of its RNA binding surface (and presumably of its RNA binding capability). It follows that the domain is not essential to the interaction between KSRP and the AU-rich sequences within the mRNAs examined. We have previously shown that a construct comprising the KH3 and KH4 domains of KSRP binds an AU-rich TNF-α sequence with high affinity, while the individual domains bind to the protein with sub-mM K_d[7]. The proposed combinatorial model of interaction we derived from these data[7] can be extended to involve KH1 and KH2. However, we report here that KH1 interacts with AU-rich sequences with an affinity substantially lower than that of the other KH domains, consistently with its reported specificity for GU-rich sequences [33]. Furthermore the length of several of the putative binding sequences fit three, not four, KH domains. It seems likely that the role of KH1 in the degradation of the mRNAs identified by Ruggiero and colleagues[10] is to connect KSRP-mediated AMD to extra cellular regulatory pathways rather than to participate in ARE binding.

AKT activation induces a conformational change of KSRP KH1 through the phosphorylation of Ser193. KH1 unfolds and creates a binding site for the predominantly nuclear 14-3-3ζ. Interaction with 14-3-3 has been shown to change the subcellular localization of TTP, a well studied mRNA degradation factor, while interaction with the 14-3-3ζ has been reported to lead to nuclear localization of PKUα protein[34] and of the actin-binding protein myopodin[35]. We show that in KSRP regulation, phosphorylation of Ser193 leads to nuclear retention of the protein by 14-3-3ζ: our analysis of the nuclear/

cytoplasmatic partitioning of the protein shows that activation of AKT leads to nuclear localization of KSRP. This effect is abolished by mutation of Ser193 by alanine and strongly reduced by co-expression of difopein together with myrAKT1. Further, nuclear/cytoplasmic partition of the protein is observed in an NLS independent fashion. How does this mechanism relate to an impairment of exosome recruitment? The interaction between KSRP and the exosome has been reported to involve several domains within the protein as well as several exosomal components[6,36,37] and is probably a combination of direct and indirect interactions within a large multi-component complex. Localization of KSRP into the nucleus and the disruption of the correct structural setting would impair protein-exosome interaction.

In the model described above the phosphorylated KSRP localizes to the nucleus and is no longer available to recruit the mRNA degradation machinery. KSRP is a multi-functional protein involved at several levels of mRNA regulation including mRNA splicing and mRNA localization[38,39]. The role of KH1 in the nuclear localization of KSRP is linked to the action of a specific kinase and influences the stability of a defined subset of mRNAs.

In this work we have used NMR and other biophysical tools to characterize a phosphorylation-mediated conformational change and to elucidate a new 14-3-3 mediated regulatory mechanism. In the past few years efforts have been made to link post-transcriptional regulatory activities to phosphorylation-mediated signaling pathways. The direct structural characterization of a phosphorylation-mediated rearrangement is an important step in understanding these processes at a molecular level and indicates that an unexpectedly high level of complexity exist in the integration of signaling pathways and RNA metabolism.

METHODS

Protein, peptide and RNA oligonucleotides preparation

The preparation of the different protein samples used in this study is described in the Supplementary methods section. The KH1 peptide (GLPERSVSLTGAPES) was synthesized in-house. All RNA oligo-nucleotides were chemically synthesized (Curevac) and used without further purification.

CD spectroscopy—All CD spectra were recorded on Jasco J-715 spectropolarimeter equipped with a PTC-348 Peltier temperature-control system. Thermal unfolding was monitored between 5 °C and 90 °C, 15 °C and 95 °C or 15 °C and 90 °C, depending on the constructs. Temperature was increased at a rate of 1 °C per min and unfolding was monitored by recording the signal at 220 nm. Reversibility was assessed by cooling to 5 °C or 15 °C at the same rate. Protein concentrations were 2-3 μM in 10 mM Tris-HCl buffer (pH 7.4), 100 mM NaCl, 1 mM TCEP. The data were fit to a two-state (native-denatured) model with *in-house* software as described[40]. For the KH12 construct two independent unfolding transitions were postulated.

NMR spectroscopy—The preparation of the NMR samples, the recording and processing of NMR spectra, the assignment of the backbone resonances and the measurament and analysis of ^{15}N relaxation parameters (T_1, T_2 and {^{1}H}-^{15}N NOE) are described in the Supplementary Methods section. The thermal stability of the domains was monitored by recording ^{15}N-HSQC spectra at 3 °C intervals between 27 °C and 69 °C and is also described in detail in the Supplementary Methods section. In all cases, the protein unfolding was fully reversible.

KH1–RNA complex formation was followed by acquiring ^{15}N-HSQC spectra during titrations of 5′-UAUUUA-3′ and 5′-UAUUAU-3′ RNAs into a sample of 25 μM ^{15}N-labeled

KH domains in 10 mM Tris-HCl buffer (pH 7.4), 100 mM NaCl, 1 mM TCEP, at 27°C. The analysis of the data is described in the Supplementary Methods section.

Structure calculation and analysis—Structure calculations were performed with ARIA 1.241 using dihedral restraints obtained from experimentally measured scalar couplings (ϕ)[42] or from chemical-shift-based TALOS database (ϕ/φ)43 and experimental distance restraints (Table 1) derived from NOE peak lists compiled in SPARKY44 and integrated with XEASY[45]. H-bond constraints were added when identified by structural analysis (MOLMOL)[46] in at least 15 of the 20 preliminary structures. The low stability of the domain prevented us to extract information on the backbone amide protection parameters from H_2O/D_2O exchange experiments.

Two hundred randomized conformers underwent simulated annealing with a standard CNS protocol as described[47]. The 25 lowest energy structures were water refined[51] and the structural statistics are shown in Table 1. Structure quality was evaluated by using PROCHECK-NMR[48]. 98.6% of residues were in the most favoured/additionally allowed regions, 0.5% in the generously allowed regions and 0.9% in the disallowed regions. MOLMOL[46] was used to visualize the structure and to create figures. CLUSTALX[49] was used for multiple sequence alignment. DALI (http://www.ebi.ac.uk/dali/)[20] was used to search the PDB for closely related structures while the search of loop-turns structurally similar to the N-terminal extension within the SCOP40 domain database was undertaken using a local structure-based alphabet[21,22].

KH1 phosphorylation and de-phosphorylation and KH1 peptide phosphorylation—300 μl of 100 μM $KH1_{130–218}$ construct were phosphorylated using 1 μg of recombinant active AKT1 enzyme (Upstate Inc.). The reaction was carried out at 37°C for 48 hours and phosphorylated (~90%) and non-phosphorylated proteins were separated by gel filtration on a superdex 75 10/300GL column (GE Healthcare).

The identity of the two protein peaks was confirmed by mass spectrometry and the samples were buffer exchanged into 10 mM Tris-HCl pH 7.4, 50 mM NaCl, 1mM TCEP prior to NMR analysis. After recording the NMR spectra, phosphorylated KH1 was treated with 100 Units of λ protein phosphatase (New England Biolabs) for 60 minutes at 37 °C. The de-phosphorylated sample was purified by gel filtration as described above and analyzed by mass spectrometry. The two controls (heat-inactivated AKT1 and S193A mutant) were treated as described above.

The KH1-derived peptide was phosphorylated using AKT kinase and a protocol analogous to the one used for full length KH1. Phosphorylated peptide was then purified by reverse phase HPLC using a Zorbax C-18 column and employing a linear gradient of acidified acetonitrile from 5 to 60% over 40 minutes. The phosphorylated peptide was lyophilized and analyzed by mass spectrometry. A second peptide containing the serine-to-alanine mutation previously outlined was not phosphorylated in a control reaction.

Prior to mass spectrometry all protein samples were desalted using C18 ZipTips (Millipore, Watford, UK). They were then analyzed by flow injection on a MictoTOF-Q mass spectrometer (Bruker, Coventry, UK) using an electro spray source operated in positive ion mode. Summed spectra were deconvoluted using the maximum entropy module of the Data Analysis software suite supplied by Bruker.

Isothermal titration calorimetry—ITC experiments were carried out using a VP-ITC microcalorimeter (Microcal). Data was analyzed using the Origin 7.0-based software provided by the manufacturers. Briefly, 200 μM 14-3-3ζ was dialyzed in 10mM Tris pH 7.4,

50 mM NaCl, 1mM TCEP was titrated with 2mM YGLPERSVS$_p$LTGAPES KH1-derived peptides (phosphorylated and non, from the Department of Biochemistry, University of Bristol) in the dialysis buffer. All experiments were performed at 30°C.

Sub-cellular localization of KSRP—Exponentially growing mock-αT3-1 or αT3-1-myrAKT1 cells were collected and resuspended in buffer A (10 mMTris-HCl, pH 7.6, 1mM MgOAc, 2mM DTT, 1x Complete® and 0.1 mM PMSF). Cells were mechanically disrupted and nuclear pellet collected by centrifugation (15 min at 500g) and extracted in 450 mM NaCl, 50 mM Tris-HCl pH 8.0, 1.5 mM MgOAc, 1.5 mM KOAc and 0.5% NP-40. S100 extracts were prepared from supernatants6. Both nuclear and S100 extracts were diluted to a 150 mM salt and 0.5% NP-40 concentrations. FlagKH1-4 (aa 130-525 of the human KSRP coding sequence) and Flag-KSRP constructs have been utilized previously6,9. The plasmid expressing difopein has been described previously. Nucleo-cytoplasmic extracts from transiently transfected HEK293 cells were prepared using the NE-PER®reagents (Pierce).

Accession codes

Protein Data Bank: Coordinates of the best 25 conformers of KH1$_{130–218}$ domain from KSRP are available with an accession code 2OPU.

Supplementary Material

Refer to Web version on PubMed Central for supplementary material.

Acknowledgments

I.D.M. was supported by European Molecular Biology Organization (EMBO), fellowship number 240-2005. The work of R.G. is supported by a grant from the Italian AIRC and I.S.S, while P.B. is a recipient of a Senior Scholar Consultancy Grant from A.I.C.F. The work of R.G. and P.B. is also supported by the Italian CIPE-2007. We would like to thank Drs J. Kleinjung and A. Pandini for the fragment-based search SCOP40 database, Dr C. De Chiara, for advice on the ARIA protocols, Dr A. Oreggioni for his help in recording spectra, Dr I. Taylor for checking the oligomerisation state of protein constructs by MALLS. We would like to thank Dr K. Rittinger (MRC National Institute for Medical Research, London, UK) for the gift of the GST-14-3-3 expression vector and for help in recording the ITC measurements and Dr M. Lalle (Istituto Superiore di Sanita', Rome, Italy) for the gift of the difopein expression plasmid. Finally we would like to thank Peter Fletcher (MRC National Institute for Medical Research, London, UK) for the synthesis of many of the KH1 peptides. All NMR spectra were recorded at the MRC Biomedical NMR centre.

REFERENCES

1. Audic Y, Hartley RS. Post-transcriptional regulation in cancer. Biol. Cell 2004;96:479–498. [PubMed: 15380615]
2. Kontoyannis D, Pasparakis M, Pizarro TT, Cominelli F, Kollias G. Impaired on/off regulation of TNF biosynthesis in mice lacking TNF AU-rich elements: implications for joint and gut-associated immunopathologies. Immunity 1999;10:387–398. [PubMed: 10204494]
3. Barreau C, Paillard L, Osborne HB. AU-rich elements and associated factors: are there unifying principles? Nucleic Acids Res 2006;33:7138–7150. [PubMed: 16391004]
4. Pullmann R, et al. Analysis of turnover and translation regulatory RNA-binding protein expression through binding to cognate mRNAs. Mol. Cell. Biol 2007;27:6265–6278. [PubMed: 17620417]
5. Chen C-Y, et al. AU binding proteins recruit the exosome to degrade ARE-containing mRNAs. Cell 2001;107:451–464. [PubMed: 11719186]
6. Gherzi R, et al. A KH domain RNA binding protein, KSRP, promotes ARE-directed mRNA turnover by recruiting the degradation machinery. Mol. Cell 2004;14:571–583. [PubMed: 15175153]

7. García-Mayoral MF, et al. The structure of the C-terminal KH domains of KSRP reveals a non canonical motif important for mRNA degradation. Structure 2007;15:485–498. [PubMed: 17437720]
8. Briata, et al. p38-dependent phosphorylation of the mRNA decay-promoting factor KSRP controls the stability of select myogenic transcripts. Mol. Cell 2005;20:891–903. [PubMed: 16364914]
9. Gherzi R, et al. The RNA-binding protein KSRP promotes decay of β-catenin mRNA and is inactivated by PI3K-AKT signaling. PLoS Biol 2006;5:82–95.
10. Ruggiero T, et al. Identification of a set of KSRP target transcripts up-regulated by PI3K-AKT signaling. BMC Molecular Biology 2007;8:28–43. [PubMed: 17437629]
11. Yaffe MB, et al. The structural basis for 14-3-3:phospho-peptide binding specificity. Cell 1997;91:961–971. [PubMed: 9428519]
12. Mackintosh C. Dynamic interactions between 14-3-3 proteins and phospho-proteins regulate diverse cellular processes. Biochem. J 2004;381:329–342. [PubMed: 15167810]
13. Aitken A. 14-3-3 proteins: a historic overview. Semin. Cancer Biol 2006;16:162–172. [PubMed: 16678438]
14. Gardino AK, Smerdon SJ, Yaffe MB. Structural determinants of 14-3-3 binding specificities and regulation of sub cellular localization of 14-3-3-ligand complexes: a comparison of the X-ray crystal structures of all human 14-3-3 isoforms. Semin. Cancer. Biol 2006;16:173–182. [PubMed: 16678437]
15. Stoecklin G, et al. MK2-induced tristetraprolin:14-3-3 complexes prevent stress granule association and ARE-mRNA decay. EMBO J 2004;23:1313–1324. [PubMed: 15014438]
16. Johnson BA, Stehn JR, Yaffe MB, Blackwell TK. Cytoplasmic localization of tristetraprolin involves 14-3-3-dependent and -independent mechanisms. J. Biol. Chem 2002;277:18029–18036. [PubMed: 11886850]
17. Musco G, et al. The solution structure of the first KH domain of FMR1, the protein responsible for the fragile X syndrome. Nat. Struct. Mol. Biol 1997;4:712–716.
18. Baber JL, Levens D, Libutti D, Tjandra N. Chemical shift mapped DNA-binding sites and ^{15}N relaxation analysis of the C-terminal KH domain of heterogeneous nuclear ribonucleoprotein K. Biochemistry 2000;39:6022–6032. [PubMed: 10821674]
19. Ramos, et al. Role of dimerization in KH/RNA complexes: the example of Nova KH3. Biochemistry 2002;41:4193–4201. [PubMed: 11914064]
20. Holm L, Sander C. Protein structure comparison by alignment of distance matrices. J. Mol. Biol 1993;233:123–138. [PubMed: 8377180]
21. Camproux AC, Gautier R, Tufféry P. A hidden markov model derived structural alphabet for proteins. J. Mol. Biol 2004;339:591–605. [PubMed: 15147844]
22. Pandini A, Bonati L, Fraternali F, Kleinjung J. MinSet: a general approach to derive maximally representative database subsets by using fragment dictionaries and its application to the SCOP database. Bioinformatics 2007;23:515–516. [PubMed: 17204463]
23. Beuth B, Pennell S, Arnvig KB, Martin SR, Taylor IA. Structure of a *Mycobacterium tuberculosis* NusA-RNA complex. EMBO J 2005;24:3576–3587. [PubMed: 16193062]
24. Git A, Standart N. The KH domains of *Xenopus* Vg1RBP mediate RNA binding and self-association. RNA 2002;8:1319–1333. [PubMed: 12403469]
25. Valverde R, Pozdnyakova I, Kajander T, Venkatraman J, Regan L. Fragile X mental retardation syndrome: structure of the KH1-KH2 domains of fragile X mental retardation protein. Structure 2007;15:1090–1098. 2007. [PubMed: 17850748]
26. Bernadó P, et al. Interpretation of NMR relaxation properties of Pin1, a two-domain protein, based on Brownian dynamic simulations. J. Biomol NMR 2004;29:21–35. [PubMed: 15017137]
27. Lewis HA, et al. Sequence-specific RNA binding by a Nova KH domain: Implications for paraneoplastic disease and the fragile X syndrome. Cell 2000;100:323–332. [PubMed: 10676814]
28. Schanda P, Brutscher B. Very fast two-dimensional NMR spectroscopy for real-time investigation of dynamic events in proteins on the time scale of seconds. J. Am. Chem. Soc 2005;127:8014–8015. [PubMed: 15926816]

UKPMC Funders Group Author Manuscript

29. Sreerama N, Venyaminov SY, Woody RW. Estimation of protein secondary structure from circular dichroism spectra: inclusion of denatured proteins with native proteins in the analysis. Anal. Biochem 2000;287:243–251. [PubMed: 11112270]
30. Masters SC, Fu H. 14-3-3 proteins mediate an essential anti-apoptotic signal. J. Biol. Chem 2001;276:45193–45200. [PubMed: 11577088]
31. Johnson LN, O'Reilly M. Control by phosphorylation. Curr. Opin. Struct. Biol 1996;6:762–769. [PubMed: 8994876]
32. Messías AC, Harnisch C, Ostareck-Lederer A, Sattler M, Ostareck DH. The DICE-binding activity of KH domain 3 of hnRNP K is affected by c-src-mediated tyrosine phosphorylation. J. Mol. Biol 2006;361:470–481. [PubMed: 16854432]
33. García-Mayoral MF, Díaz-Moreno I, Hollingworth D, Ramos A. The sequence selectivity of KSRP explains its flexibility in the recognition of the RNA targets. Nucleic Acid Res 2008;36:5290–5296. [PubMed: 18684992]
34. Zhang S, Xing H, Musli AJ. Nuclear localization of protein kinase U-α is regulated by 14-3-3. J. Biol. Chem 1999;274:24865–24872. [PubMed: 10455159]
35. Faul C, Hüttelmaier, Oh J, Hachet V, Singer RH, Mundel P. Promotion of importin α-mediated nuclear import by the phosphorylation-dependent binding of cargo protein to 14-3-3. J. Cell Biol 2005;169:415–424. [PubMed: 15883195]
36. Chou CF, et al. Tethering KSRP, a decay-promoting AU-rich element-binding protein, to mRNAs elicits mRNA decay. Mol. Cell. Biol 2006;26:3695–3706. [PubMed: 16648466]
37. Lin WJ, Duffy A, Chen C-Y. Localization of AU-rich element-containing mRNA in cytoplasmic granules containing exosome subunits. J. Biol. Chem 2007;282:19958–19968. [PubMed: 17470429]
38. Markovtsov V, et al. Cooperative assembly of an hnRNP complex induced by a tissue-specific homolog of poly-pyrimidine tract binding protein. Mol. Cell. Biol 2000;20:7463–7479. [PubMed: 11003644]
39. Blichenberg A, et al. Identification of a *cis*-acting dendritic targeting element in MAP2 mRNAs. J. Neurosci 1999;19:8818–8829. [PubMed: 10516301]
40. Masino L, Martin SR, Bayley PM. Ligand binding and thermodynamic stability of a multidomain protein, calmodulin. Prot. Sci 2000;9:1519–1529.
41. Linge JP, O'Donoghue SI, Nilges M. Automated asignment of ambiguous nuclear overhauser effects with ARIA. Methods Enzymol 2001;339:71–90. [PubMed: 11462826]
42. Ye JQ, Mayer KL, Mayer MR, Stone MJ. NMR solution structure and backbone dynamics of the CC chemokine eotaxin-3. Biochemistry 2001;40:7820–7831. [PubMed: 11425309]
43. Cornilescu G, Delaglio F, Bax A. Protein backbone angle restraints from searching a database for chemical shift and sequence homology. J. Biomol. NMR 1999;13:289–302. [PubMed: 10212987]
44. Goddard, TD.; Kneller, DG. SPARKY. University of California; San Francisco: 2004.
45. Bartels C, Xia T-H, Billeter M, Güntert P, Wüthrich K. The program XEASY for computer-supported NMR spectral analysis of biological macromolecules. J. Biomol. NMR 1995;5:1–10. [PubMed: 7881269]
46. Koradi R, Billeter M, Wüthrich K. MOLMOL: a program for display and analysis of macromolecular structures. J. Mol. Graph 1996;14:51–55. [PubMed: 8744573]
47. De Chiara C, et al. The AXH domain adopts alternative folds: The solution structure of HBP1 AXH. Structure 2005;13:743–753. [PubMed: 15893665]
48. Laskowski RA, Rullman JA, MacArthur MW, Kaptein R, Thorton JM. AQUA and PROCHECK-NMR: programs for checking the quality of protein structures solved by NMR. J. Biomol. NMR 1996;8:477–486. [PubMed: 9008363]
49. Jeanmougin F, Thompson JD, Gouy M, Higgins DG, Gibson TJ. Multiple sequence alignment with Clustal X. Trends Biochem. Sci 1998;23:403–405. [PubMed: 9810230]

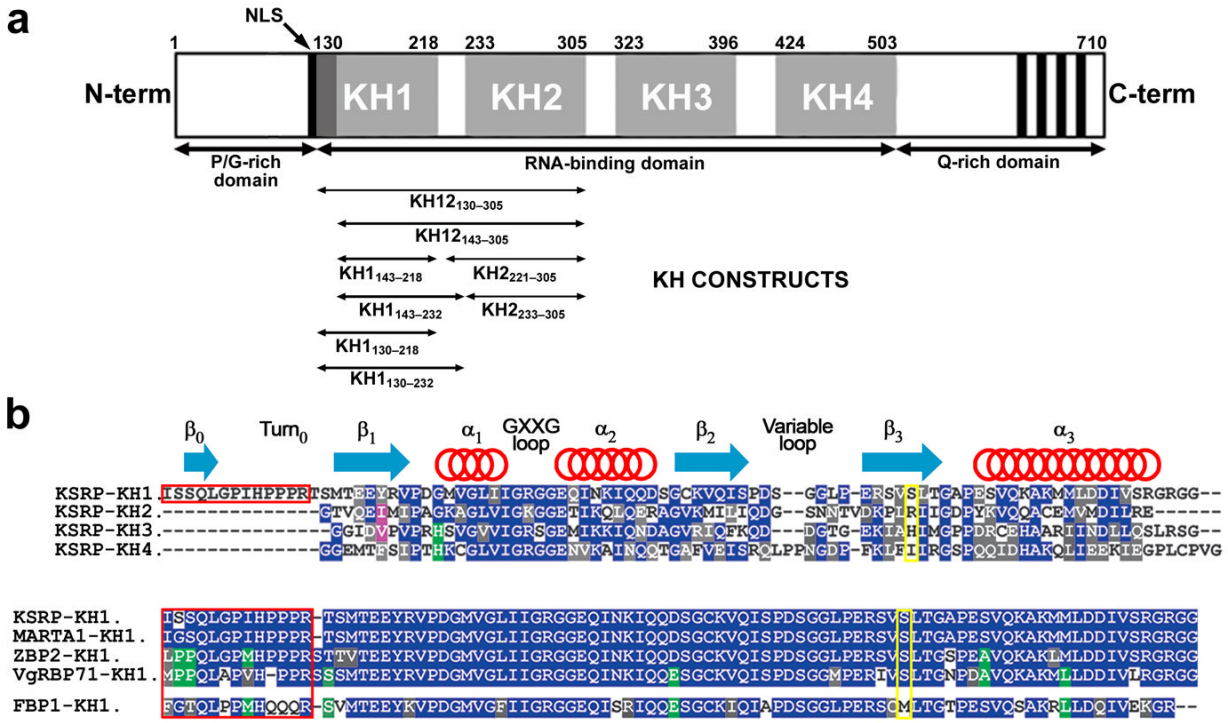

Figure 1. Domain structure and sequence alignment of the KSRP protein

(a) Domain organization of KSRP (top) and constructs used in this study (below). KH domains are indicated by light grey shadowing. The dark grey shadowing N-terminal to KH1 indicates an extension of the classical KH fold. **(b)** Sequence alignment of the four KH domains of KSRP (top) and of KH1 domains in the FBP2/FBP family (bottom). The rat (*Rattus norvegicus*, MARTA1), chicken (*Gallus gallus*, ZBP2) and frog (*Xenopus laevis*, VgRBP71) homologues and the human FUSE binding protein (FBP1), are aligned with human KSRP. Strictly conserved residues in two or more domains are colored in blue and green; conservative substitutions of hydrophobic and polar residues are marked in gray and purple. Yellow boxes point out the position of Ser193; red boxes define the boundaries of the N-terminal extension at KH1. Secondary structure elements and loops are also shown. The FBP2 family sequence alignment indicates that a 13-amino acid stretch amino-terminal to the core KH1 domain is conserved in the FBP2 but not in the FBP family.

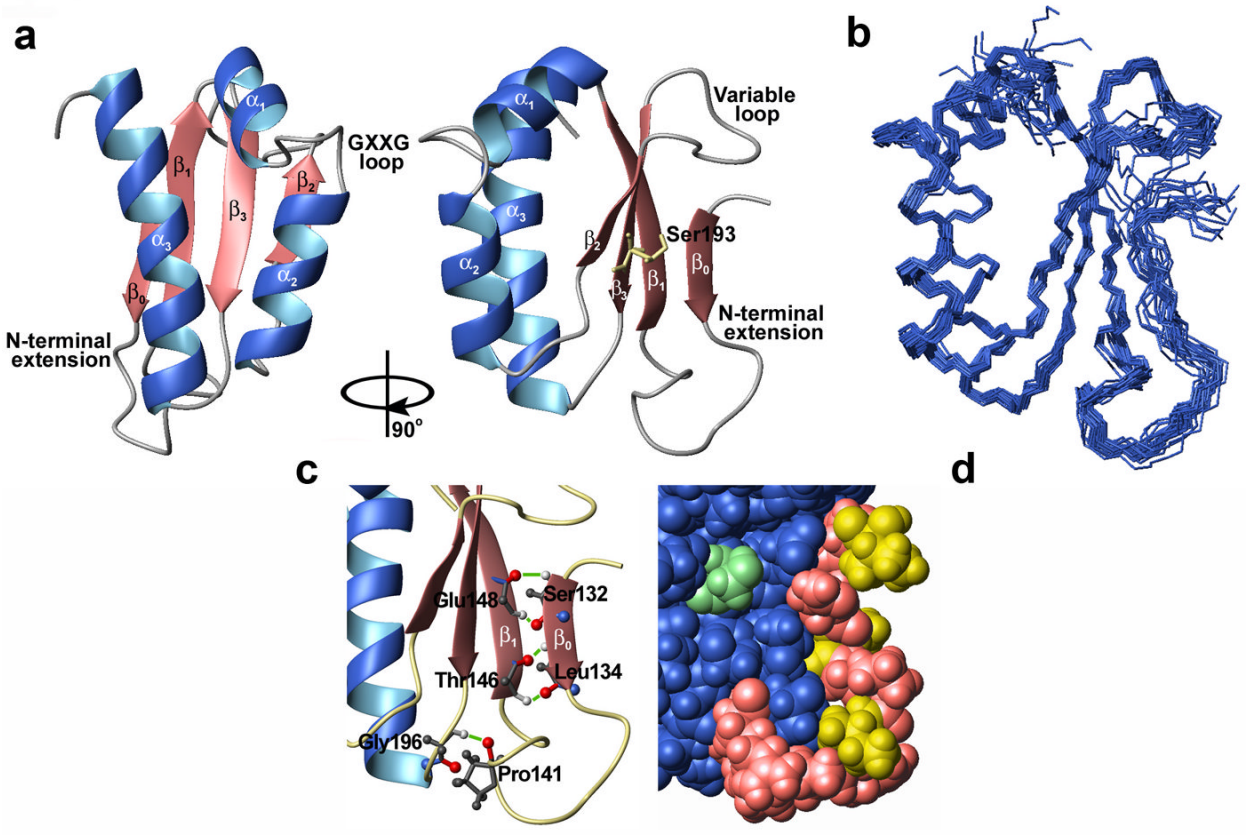

Figure 2. High resolution solution structure of KSRP KH1 domain

(a) 90° rotated ribbon representations of the solution structure of the KSRP $KH1_{130–218}$ domain. The side-chain of Ser193 on the β_3 is displayed in yellow. The N-terminal extension folds back to join the antiparallel β sheet. **(b)** Superposition of the KH1 C^{α} trace for the 25 lowest energy conformers plus the average structure. **(c)** Close-up of the β_0 - β_1 and of the $turn_0$-α_3 interactions. The hydrogen bonds between Ser132 HN and Glu148 O, Ser132 O and Glu148 HN, Leu134 HN and Thr146 O, Leu134 O and Thr146 HN, Pro141 O and Gly196 HN are indicated by green lines. The side-chains of Pro141 and Gly196 are displayed. **(d)** A space-filling (CPK) representation of the close-up in panel (c). The N-tail extension is in pink with hydrophobic amino acids in yellow. The classical KH fold is in blue with the Ser193 residue marked in green. The interaction between the two elements (including the Proline-rich loop) buries ~980$Å^2$ of exposed surface.

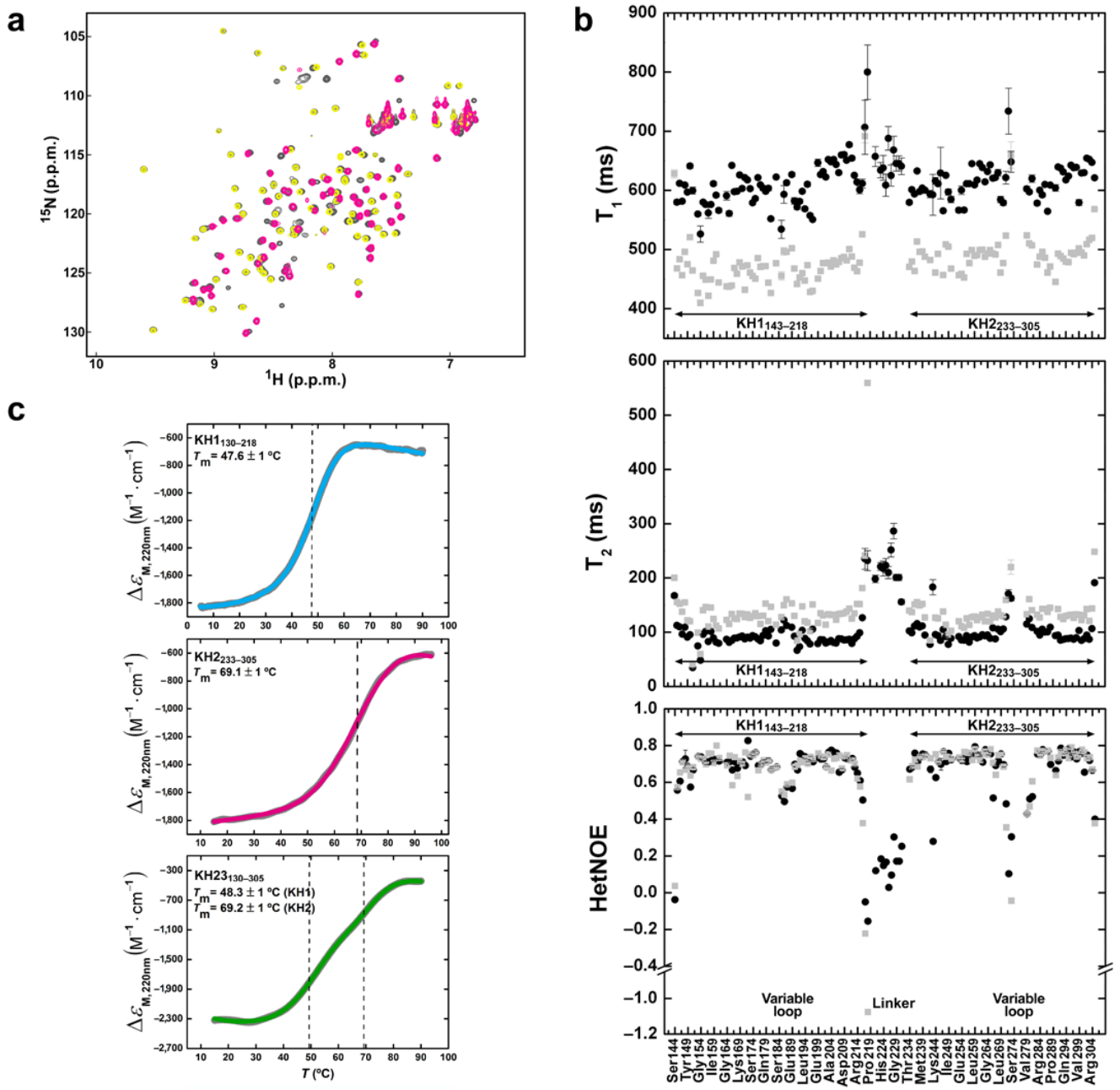

Figure 3. KH1 and KH2 do not make contact

a) Superimposition of ^{15}N-HSQC spectra of KH1$_{143–218}$ (yellow), KH2$_{233-305}$ (magenta) and KH12$_{143–305}$ (gray). No appreciable chemical-shift perturbations ($\Delta\delta_{avg}$ > 0.02 ppm) are observed between corresponding resonances in the one- and two-domain constructs. The larger of these shifts are observed for a small (4-5) set of resonances in KH2, and we can attribute them to very transient contacts between KH2 and the flexible linker. The comparison of the spectra of KH1, KH2 and KH12 indicates that the two domains are not interacting. **b)** Comparison of the backbone ^{15}N T_1, T_2 and ^{15}N{^{1}H} NOE measurements for KH1$_{143–218}$ and KH2$_{233-305}$ (gray) and KH12$_{143–305}$ (black). The trend of relaxation parameters along the sequence is the same in the isolated and two-domain constructs. **(c)** 220 nm CD signal of KH1$_{130–218}$, KH2$_{233–305}$ and KH12$_{130–305}$ recorded during a thermal

denaturation experiment. The fitted curves of unfolding are represented in cyan, magenta and green, respectively and are superimposed on experimental data in gray. Protein unfolding is reversible in all cases and transition mid-points, marked by a dashed line, do not change substantial in the two domain construct.

UKPMC Funders Group Author Manuscript

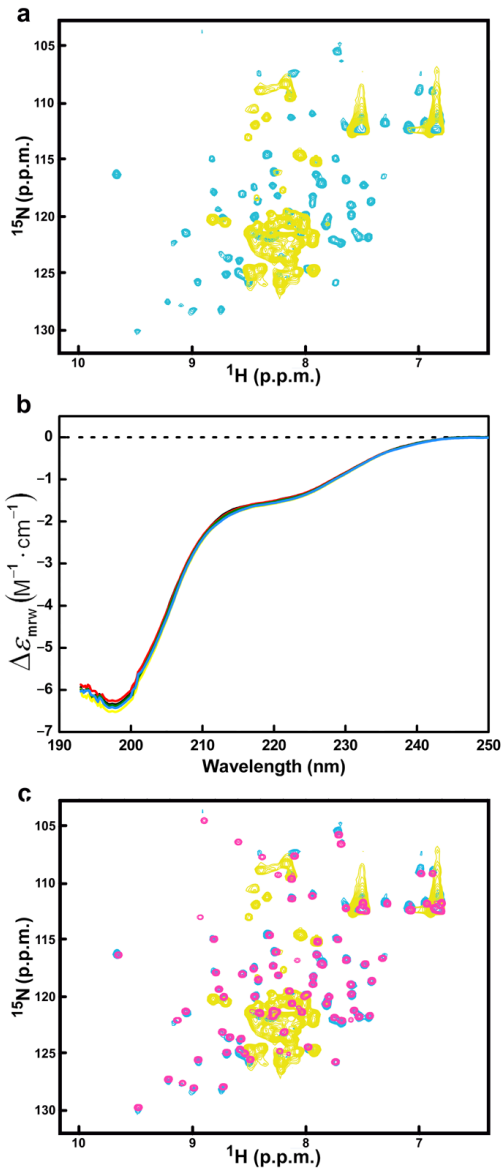

Figure 4. KH1 phosphorylation by AKT kinase

(a) Superimposition of SOFAST ^{15}N-HMQC spectra of the HPLC-purified non-phospho (cyan) and phospho (yellow) KH1. The phospho-KH1 is unfolded. **(b)** Superimposition of CD spectra of phospho-KH1 recorded at 20 (black), 40 (blue), 60 (green), 80 (red) and 95 (yellow) °C. The spectra do not change substantially at increasing temperatures. **(c)** Superimposition of SOFAST ^{15}N-HMQC spectra of non-phospho (cyan), phospho (yellow) and de-phospho (magenta) KH1 domain. KH1 de-phosphorylation results in refolding of the domain.

UKPMC Funders Group Author Manuscript

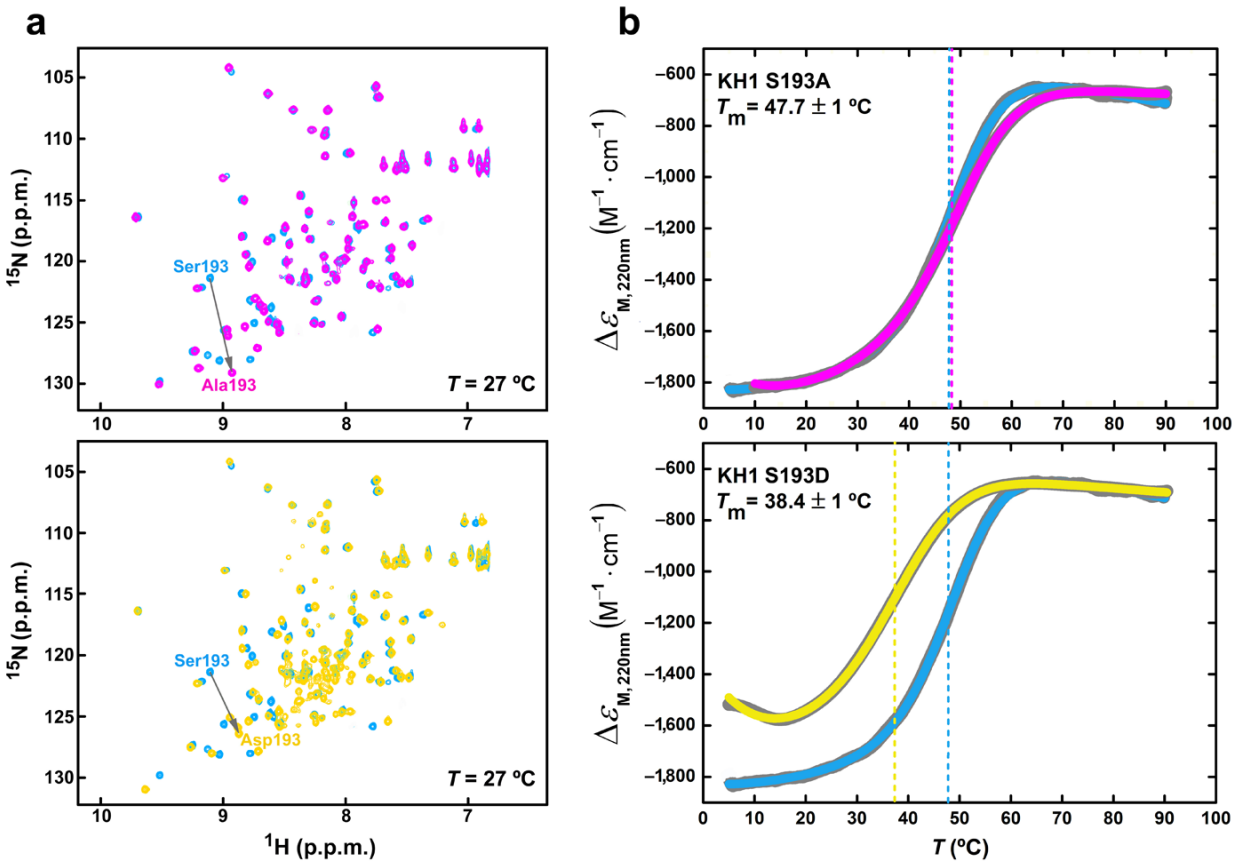

Figure 5. KH1 S193A and S193D mutants

(a) Superimpositions of ^{15}N-HSQC spectra of KH1 *wild type* (cyan) to S193A (magenta) (top) and *wild type* (cyan) to S193D (yellow) (bottom). With the exception of the resonances of residues close to Ser193, the S193A spectrum resembles the *wild type* one. Contrarily, S193D mutant is partially unfolded with both native and denatured, forms in equilibrium at 27 °C. The shift of the amide resonance of residue 193 is highlighted by arrows in the two superimpositions. **(b)** Superimposition of the 220 nm CD signals of KH1 *wild type* and S193A (top) and *wild type* and S193D (bottom) recorded during a temperature unfolding experiment. The fitted curves are colored as in (a) and superimposed on the experimental data (grey). For all constructs, protein unfolding is reversible with midpoints indicated by dashed lines. The S193D mutant is characterized by a lower T_m value compared with KH1 *wild type* and S193A mutant.

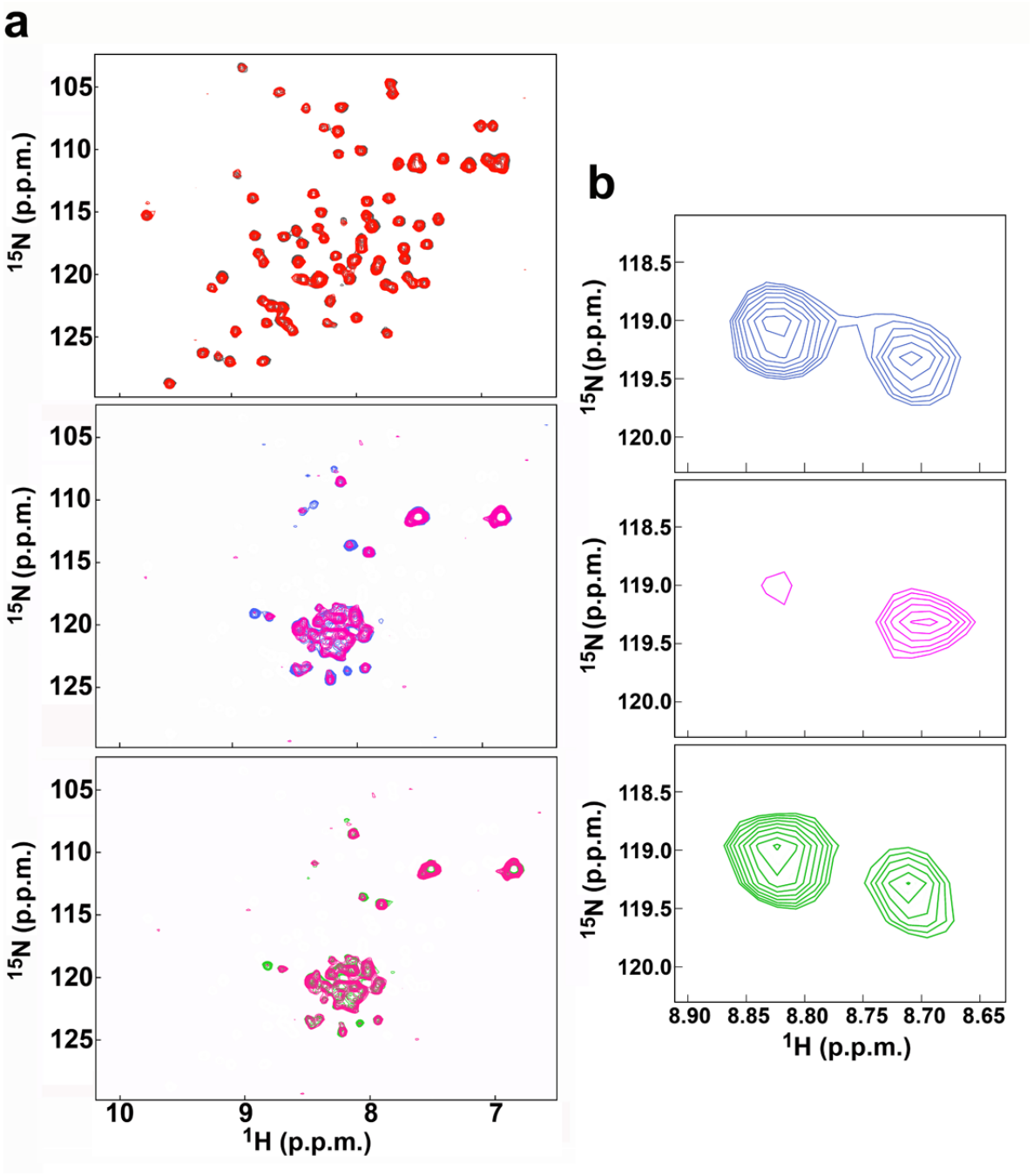

Figure 6. KH1–14-3-3ζ interaction

(a) Top - Superimposition of SOFAST ^{15}N-HMQC spectra of 15 μM KSRP KH1 (black) and KH1+14-3-3 1:2 ratio (red). No appreciable change is observed in the spectrum of the domain. Middle - Superimposition of SOFAST ^{15}N-HMQC spectra of 15 μM phospho-KH1 (cyan) and phospho-KH1+14-3-3 1:2 ratio (magenta). Selected resonances broaden substantially. Bottom - Superimposition of SOFAST ^{15}N-HMQC spectra of 15 μM phospho-KH1+14-3-3 1:2 ratio (magenta) and phospho-KH1+14-3-3+KH1 phospho-peptide 1:2:10 ratios (green). The selective broadening caused by the interaction with phospho-KH1 is reversed by addition of the peptide, indicating that the short peptide compete effectively with the full-length domain. **(b)** Detail of SOFAST ^{15}N-HMQC spectra of phospho-KH1

(top), phospho-KH1+14-3-3 1:2 ratio (middle) and phospho-KH1+14-3-3+KH1 phospho-peptide 1:2:10 ratios (bottom). Selective broadening of one of the two peaks is reversed by adding the peptide.

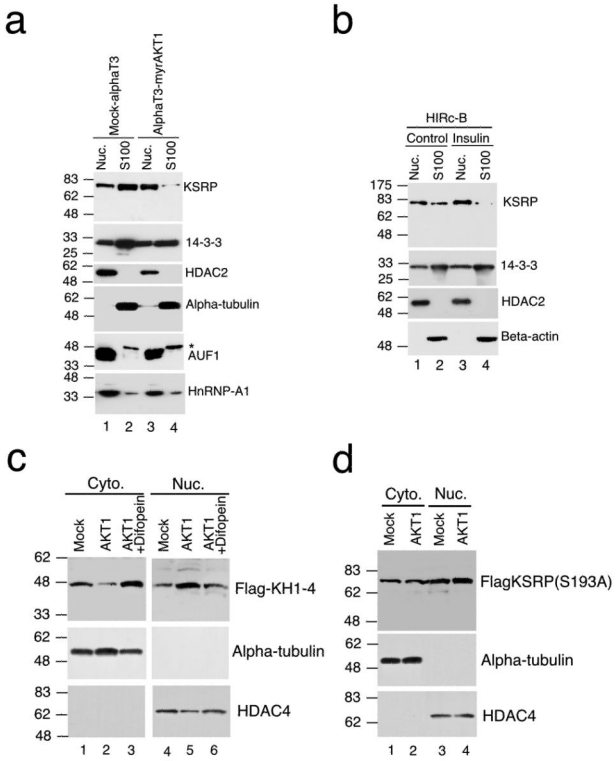

Figure 7. Sub-cellular KSRP localization

(a) Immunoblot analysis of either nuclear or S100 cytoplasmic extracts from either mock-αT3-1 and αT3-1-myrAKT1 cells with the specified antibodies. Asterisks mark the position of a non-specific band in anti-AUF1 immunoblot. **(b)** Immunoblot analysis of either nuclear or cytoplasmic extract from either control or insulin (10^{-6} M, 1h)-treated HIRc-B cells using the indicated antibodies. **(c)** Immunoblot analysis (antibodies are indicated) of either nuclear or cytoplasmic extracts from HEK293 cells transiently transfected with Flag-KH1-4 and either empty vector (mock) or myrAKT1 (AKT1) or myrAKT1 together with difopein expression vector (AKT1+ difopein). **(d)** Immunoblot analysis (antibodies are indicated) of either nuclear or cytoplasmic extracts from HEK293 cells transiently transfected with Flag-KSRP(S193A) and either empty vector (mock) or myrAKT1 (AKT1).

Table 1

NMR and refinement statistics for protein structures

	Protein
NMR distance and dihedral constraints	
Distance constraints	
Total NOE	1815
Intra-residue	760
Inter-residue	1055
Sequential ($\|i - j\| = 1$)	392
Medium-range ($\|i - j\| < 4$)	229
Long-range ($\|i - j\| > 5$)	434
Intermolecular	
Hydrogen bonds	34
Total dihedral angle restraints	119
ϕ	76
ψ	43
Structure statistics	
Violations (mean ± s.d.)	
Distance constraints (Å)	0.022 ± 0.016
Dihedral angle constraints (°)	0.345 ± 0.147
Max. dihedral angle violation (°)	0.042 ± 0.200
Max. distance constraint violation (Å)	0.44 ± 0.49
Deviations from idealized geometry	
Bond lengths (Å)	0.0044 ± 0.0002
Bond angles (°)	0.578 ± 0.019
Impropers (°)	1.680 ± 0.119
Average pairwise r.m.s. deviation, 25 conformers (Å)	
Heavy	1.48 ± 0.25
Backbone	0.75 ± 0.16